European Journal of Radiology Open 3 (2016) 200–206

Contents lists available at ScienceDirect

European Journal of Radiology Open

journal homepage: www.elsevier.com/locate/ejro

Accuracy of unenhanced magnetic resonance angiography for the assessment of renal artery stenosis

Carmen Sebastià (MD), Alejandro D. Sotomayor (MD), Blanca Paño (MD), Rafael Salvador (MD), Marta Burrel (MD), Albert Botey* (Prof), Carlos Nicolau (MD)

CDI, Department of Radiology and Nephrology, Hospital Clinic of Barcelona, Spain

ARTICLE INFO

Article history:
Received 15 April 2016
Received in revised form 6 July 2016
Accepted 11 July 2016
Available online 4 August 2016

Keywords:
Unenhanced magnetic resonance angiography (U-MRA)
Renal artery stenosis (RAS)
Contrast-enhanced magnetic resonance angiography (CE-MRA)
Fibromuscular dysplasia (FMD)
Hypertension (HTA)

ABSTRACT

Purpose: To evaluate the accuracy of unenhanced magnetic resonance angiography (U-MRA) using balanced steady-state free precession (SSFP) sequences with inversion recovery (IR) pulses for the evaluation of renal artery stenosis.

Materials and methods: U-MRA was performed in 24 patients with suspected main renal artery stenosis. Two radiologists evaluated the quality of the imaging studies and the ability of U-MRA to identify hemodynamically significant main renal artery stenosis (RAS) defined as a stenosis ≥50% when compared to gold standard tests: contrast-enhanced magnetic resonance angiography (CE-MRA) (18 patients) or digital subtraction arteriography (DSA) (6 patients).

Results: A total of 44 main renal arteries were evaluated. Of them, 32 renal arteries could be assessed with U-MRA. When CE-MRA or DSA was used as the reference standard, nine renal arteries had hemodynamically significant RAS. U-MRA correctly identified eight out of nine arteries as having ≥50% RAS, and correctly identified 22 out of 23 arteries as not having significant RAS, with a sensitivity of 88.8%, a specificity of 95.65%, positive and negative predictive value of 88.8% and 95.65%, respectively, and an accuracy of 93.75%. Renal artery fibromuscular dysplasia (FMD) was observed in the two misclassified arteries.

Conclusion: U-MRA is a reliable diagnostic method to depict normal and stenotic main renal arteries. U-MRA can be used as an alternative to contrast-enhanced magnetic resonance angiography or computer tomography angiography in patients with renal insufficiency unless FMD is suspected.

© 2016 The Authors. Published by Elsevier Ltd. This is an open access article under the CC BY-NC-ND license (http://creativecommons.org/licenses/by-nc-nd/4.0/).

1. Introduction

Renal artery stenosis (RAS) is a well-known cause of hypertension (HTA) and is associated with progressive, decreased kidney function and renal failure. RAS has a prevalence of about 6.8% in the elderly population [1]. It is well established that the prevalence of RAS is higher in elderly patients, particularly in those with comorbid conditions such as diabetes, coronary artery disease (CAD), aortoiliac occlusive disease, or HTA [2]. Although controversial, there is general consensus that interventions to prevent the loss of renal function should be performed before there is a clinically evident decline of the renal function [3,4].

The successful implementation of this strategy requires an efficient and accurate method of screening for RAS in patients at risk. Noninvasive tools such as Doppler ultrasound, computed tomography angiography (CTA) or contrast enhanced magnetic resonance angiography (CE-MRA) have been widely applied in clinical practice for several years for the evaluation of the renal arteries and veins [5–8]. The main limitation of CTA is radiation exposure and the necessity of administration iodinated contrast media in patients with decreased renal function or previous severe allergic reaction [9,10]. In addition to the general limitations of MRI, there is a potential risk of nephrogenic systemic fibrosis (NSF) that has been associated with some gadolinium-based contrast media in patients with markedly reduced glomerular filtration [11,12]. Invasive imaging with digital subtraction angiography (DSA) is the traditional gold standard for imaging renal artery anatomy but this technique is reserved when the results of noninvasive imaging tests are inconclusive or when a renal artery revascularization is indicated [4].

Recently, unenhanced magnetic resonance angiography (U-MRA) has been re-explored as an alternative to CE-MRA for the assessment of renal artery stenosis [13–15]. Few studies have

* Corresponding author at: CDIC, Hospital Clínic, Villarroel 170, 08036 Barcelona, Spain.
E-mail address: msebasti@clinic.ub.es (C. Sebastià).

http://dx.doi.org/10.1016/j.ejro.2016.07.003
2352-0477/© 2016 The Authors. Published by Elsevier Ltd. This is an open access article under the CC BY-NC-ND license (http://creativecommons.org/licenses/by-nc-nd/4.0/).

evaluated the usefulness of balanced steady-state free precession (SSFP) combined with arterial spin labeling (ASL) for the depiction of renal vasculature [16–22]. This technique seems a good alternative to be used in cases where contrast administration is not safe.

The main goal of this study is to determine the imaging quality and accuracy of U-MRA using balanced SSFP acquisition with inversion recovery (IR) pulses (Inhance 3D inflow IR [*GE* ®]) and compare them with a gold standard tests (CE-MRA or DSA) for the evaluation of renal artery stenosis.

2. Material and methods

2.1. Patients

From February 2012 to December 2014, all of the patients who were referred for a CE-MRA of renal arteries were included in this study. A U-MRA sequence in addition to the conventional CE-MRA images was added. The Hospital Ethics Committee approved the study and informed consent was obtained from all participants. A total of 24 patients, 14 men and 10 women, were included (mean age 56 ± 18 years). The 24 patients were referred to MRA due to Doppler Ultrasound findings: 22 of them (12 patients had uncontrolled HTA, 6 patients had deterioration of the renal function) because of suspected stenosis of the main renal artery, one patient for follow up of a renal artery aneurysm not properly visible by ultrasound, and one patient for suspected RAS of a kidney graft. Participants formed a random series.

2.2. Imaging protocols

2.2.1. U-MRA parameters

All examinations were performed with a 1.5T General Electric Hdxt MR system. An 8 channel phased array body coil was used for signal reception and respiratory-triggered 3D SSFP with fat saturation pulses was also used. MRI studies were performed feet first with the patient's arms above the head. Respiratory gating technique was used to mitigate the effects of respiratory motion. SSFP U-MRA imaging was performed in the transverse plane with to cover approximately 12 cm to visualize both kidneys and anticipating that the kidneys will move up 1–2 cm during free breathing. Inversion pulses are used for background suppression by saturation of arterial and venous blood and fat. After inversion, fast imaging with steady-state data acquisition occurs. This allows the background and venous blood to reach a null point, while the fresh inflowing arterial blood that is not affected by the inversion pulse has full magnetization. The arteries generate a significantly bright signal due to the in-flow effects of the fresh blood. The technique called SPECIAL (Spectral Inversion At Lipid) was implemented to achieve good fat saturation. Parallel imaging (array spatial sensitivity encoding technique, ASSET) was used in the in-plane phase-encode direction. The scanning parameters were TR = 4.6; TE = 2.3; flip angle = 90°; TI = 1200 ms; matrix = 256 × 256; FOV = 36 × 40 cm; slice thickness = 2 mm; slice number = 50, readout bandwidth = 125.00 kHz, Nex1; and the average scan time = 1 min and 50 s.

2.2.2. CE-MRA parameters

The CE-MRA sequence was a 3D fast-spoiled gradient echo (FSPGR). The imaging sequence was performed in the coronal plane with an anatomical range that covered both kidneys and the aorta. Automatic triggering (Smart prep) was used to start the MR data acquisition when the contrast agent reached an optimal concentration in the renal arteries. This was detected by positioning a tracker in the aorta, just superior to the renal arteries. The maximum monitoring period was 40 s. Breathing suspension was required for the duration of MR data acquisition. Parallel imaging (ASSET) was used in the in-plane phase-encode direction with an acceleration factor of 2. The MR imaging parameters were as follows: TE = 1.5 ms; TR = 4.4 ms; flip angle = 30°; receiver band width 41 Hz/pixel; FOV = 36 × 40.0; slice thickness = 2.8 mm; locations per slab = 38; frequency matrix = 320; phase matrix = 224; the phase FOV is reduced dependent on the patient's size, being a 0.8 phase FOV generally adequate. Acquisition time = 16–20 s breath-hold. Gadobutrol (GADOVIST 1.0, BAYER, Berkshire, UK) (0,1 mL/kg) was injected at a rate of 2 mL/s followed by 20 mL of saline while the smart preparation function monitored the change of signal that indicates the arrival of contrast agent.

U-MRA and CE-MRA were post-processed in a Volume Share 2 Advantage Workstation 4.4 (General Electric) using the Volume Viewer 3.1 application. Axial and coronal MIP reformations were performed in all cases.

2.2.3. Digital subtraction angiography protocol

DSA was performed with a monoplane C-arm angiography system (AXIOM Artis Forchheim, Germany). An interventional radiologist performed the study through the right femoral arterial route in all the patients. The standard protocol included an abdominal aortography using a 5F pigtail catheter and the injection of 30 mL of iodinated contrast medium at a flow rate of 15 mL/s. A selective angiography of the renal artery with suspected significant stenosis was performed with a 5F Simmons 1 or Cobra catheter or a 4F Hook catheter ands injecting 12 mL of iodinated contrast medium at a flow rate of 4 mL/s in the anteroposterior and oblique planes.

2.3. Image analysis

Two radiologists with 9 and 11 years of experience in abdominal MRI (BP and RS) independently evaluated the ability of U-MRA to visualize the renal arteries and to demonstrate main renal artery disease. Each radiologist independently reviewed source images and MIP reconstructions of the U-MRA studies. We chose to use non-automated methods for reader quantification. Reference standard tests were not available for the readers.

CE-MRA was used as a gold standard in 18 patients and DSA in 6 patients. Since the study was done in a clinical setting, DSA was chosen as the reference standard when available. DSA was performed in 6 patients with inconclusive noninvasive imaging tests (2 patients) or when a renal revascularization due to significant stenosis was indicated (4 patients). One radiologist with 15 years of experience in abdominal MR imaging evaluated the CE-MRA, and one radiologist with 16 years of experience in angioradiology evaluated the DSA. Index tests were available to the readers of the reference standard tests.

A hemodynamically significant RAS was defined as a moderate (50% to 69%) stenosis with ≥10 mmHg mean or ≥20 mmHg systolic translesional gradient, or a severe stenosis with a visually estimated diameter stenosis of 70% [4].

With the objective to evaluate the ability of U-MRA to identify hemodynamically significant stenosis the cut-offs for the index tests and the reference standard tests were graded as follows:

- No main renal artery stenosis (0)
- Main renal artery stenosis <50% (1).
- Main renal artery stenosis ≥50% (2).

In case of discrepancies between readers of the U-MRA studies, decisions were made by consensus.

The quality of the U-MRA images to visualize the renal arteries was assessed using the following subjective categories:

- Not assessable: vessels not visible or diagnostic information cannot be obtained because of severe blurring artifacts (0).
- Poor: inhomogeneous vessel signal intensity, irregular delineation of vessel borders (1).
- Good: homogeneous vessel signal intensity with slight flow artifacts, good delineation of vessel borders (2).
- Excellent: homogenous vessel signal intensity without flow artifacts, sharp and complete delineation of vessel borders (3).

Overall image quality of the study as well as of three predefined segments (main renal artery, hilar arteries and intraparenchymal arteries) was assessed.

The ability to depict accessory or polar arteries and findings such as dissection or aneurysm of the renal arteries were also recorded.

2.4. Statistical analisis

Statistical analyses were performed using PASW Statistics software version 18.0.0.

The sensitivity, specificity, positive predictive value (PPV) and negative predictive value (NPV) and accuracy of U-MRA for the detection of hemodynamically significant main RAS (stenosis ≥50%) in assessable main RAS was calculated using the gold standard studies (DSA or CE-MRA) as the reference.

Means, standard deviations, and medians for the overall quality of the study and in each of the predefined segments were performed.

Kappa statistics were used to evaluate interobserver variability with the following interpretation. A κ value of 0.01–0.20 indicate low agreement; from 0.21 to 0.40 acceptable agreement; 0.41 to 0.60 moderate agreement; 0.61 to 0.80 good agreement; and 0.81 to 1 perfect agreement.

3. Results

A total of 44 main renal arteries were evaluated. Of them, 32 renal arteries could be assessed with U-MRA. The remaining 12 renal arteries were excluded because of renal artery stent artifact (4 arteries), respiratory movements with blurring artifacts (4 arteries), kidney shrinkage with occluded renal artery (1 artery), technical problems in renal artery graft (1 artery), and artifacts caused by aortic endoprosthesis (2 arteries). A diagram of the flow of participants is shown in Fig. 1.

Baseline demographics and clinical characteristics of the patients are shown in Table 1.

Table 1
Demographic and clinical characteristics of study population (n = 24).

Characteristics	Value
Sex	
Male	14 (58.3%)
Female	10 (41.7%)
Age	
Mean ± SD	56,45 ± 18.17
Range	24–86
Estimated GFR (ml/min)	
>60	8 (33.3%)
60–45	8 (33.3%)
45–30	2 (8.3%)
<30	6 (25%)
Common comorbilities	
Hypertension	21 (87.5%)
Diabetes mellitus	3 (12.5%)
Ischemic heart disease	4 (16.6%)
Aortoiliac occlusive disease	2 (8.3%)

In patients referred for CE-MRA, a U-MRA sequence was added to the conventional CE-MRA images. The time interval between the DSA and the U-MRA was of 2.2 months of average.

3.1. Depiction of main renal artery stenosis

There was an excellent agreement between both readers of U-MRA for the degree of renal artery stenosis (kappa: 0.83). A consensus reading was used for those arteries with discrepant readings.

The distribution of the assessment of renal artery stenosis by the consensus readings of U-MRA compared to the gold standard tests is shown in Table 2. Using CE-MRA or DSA as the reference standard, nine renal arteries had hemodynamically significant RAS. U-MRA correctly classified 8 of 9 arteries with RAS and correctly classified 22 of 23 as not having significant disease with a sensitivity of 88.8%, specificity of 95.65%, positive and negative predictive value of 88.8% and 95.65%, respectively, and an accuracy of 93.75%.

There were two clinically important misclassified arteries: one missed case of stenosis >50% on U-MRA, which was rated as stenosis <50%, and another case of overestimation of stenosis as hemodynamically significant. The two cases were in patients with renal artery FMD. In four cases there was mismatching between grades of stenosis: two of the arteries did not have artery stenosis (grade 0) but were classified as having <50% stenosis (grade 1), and the other two arteries that had <50% renal artery stenosis were considered normal (grade 0) using U-MRA. In the four cases, the controversial images corresponded to areas of kinking of the main renal arteries.

3.2. Depiction of aneurysms and accessory renal arteries

The two renal artery aneurysms in the main renal arteries were correctly described by the two readers. However none of the readers visualized a small aneurysm located in a segmental artery. None of the patients presented with renal artery dissection.

Despite the fact that accessory arteries have not been specifically analysed in this study, seven of the nine accessory arteries (three hilar and four polar arteries) visualized with the gold standard technique were also correctly evaluated. Two of the nine accessory arteries were not visualized because they arose from the lower aortic level, out of the field of view of the U-MRA.

3.3. Image quality

The quality scores for overall quality of the study and for each of the three predefined segments assigned by the two readers are summarized in Table 3. There was a good agreement between readers in the rating of the overall image quality of the study (κ: 0.65), image quality of the main renal arteries (κ: 0.69), and hilar arteries (κ: 0.65), while the agreement in the rating of the intraparenchymal arteries. U-MRA provided excellent or good image quality in the assessment of the main renal artery in 61% of the arteries according to reader 1 and 64% according to reader 2. As for intraparenchymal arteries, reader 1 and reader 2 found 43% and 34% of non-assessable arteries, respectively. The results are shown in Table 3.

4. Discussion

Recently, new U-MRA techniques, SSFP and ASL, able to identify the renal arteries with high quality have been developed by several vendors. SSFP angiography is a gradient-echo based sequence that maintains steady-state longitudinal and transverse magnetization by applying a series of equidistant radio frequency pulses. The image contrast is T2/T1 weighted, which gives blood a high signal intensity with little reliance on inflow. Three-dimensional acquisition is used to produce angiographic images with a high

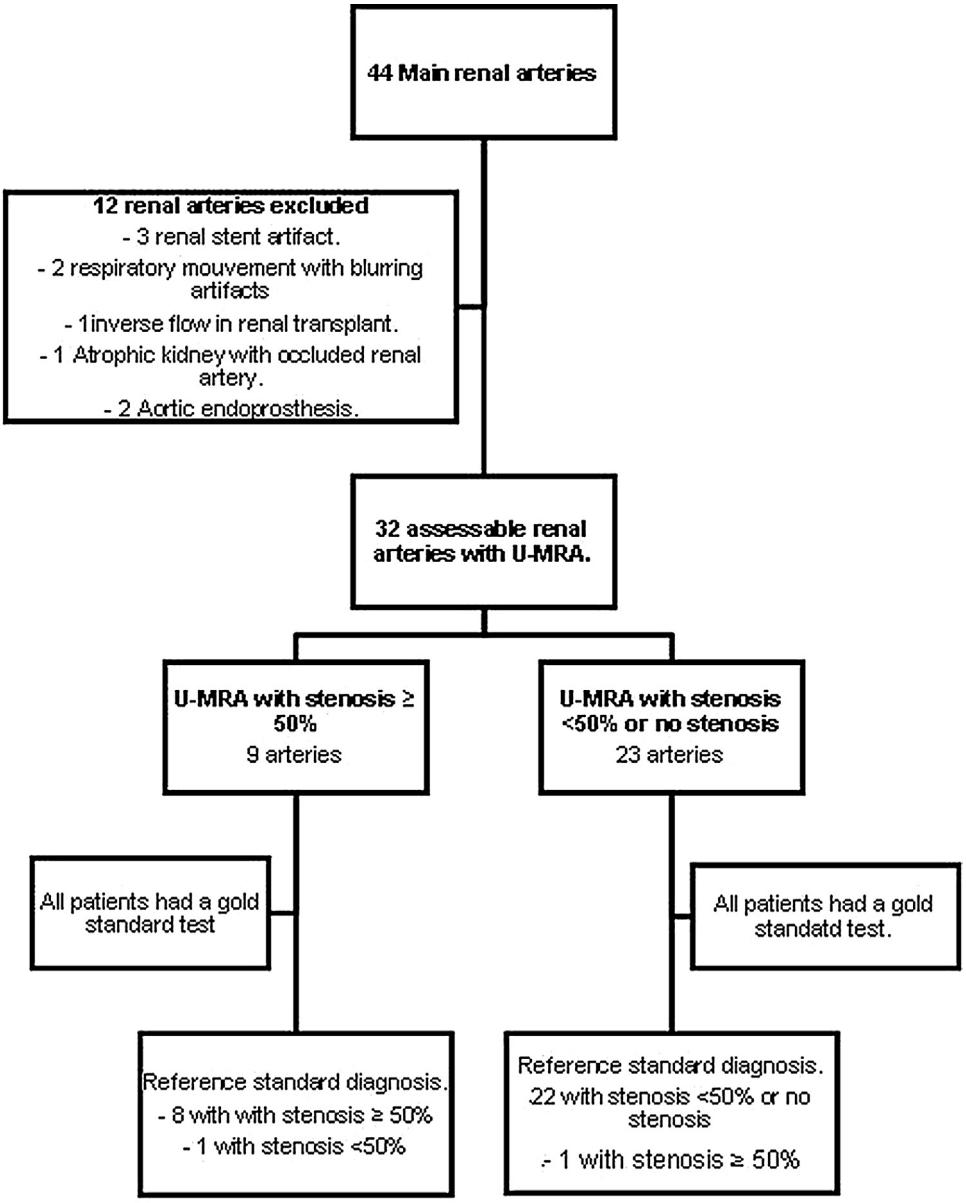

Fig. 1. Diagram of the flow of participants.

Table 2
Distribution of Renal Artery Stenosis as Assessed by Consensus using U-MRA and Gold Standard study (CE-MRA or DSA) and Diagnostic Accuracy of U-MRA.

		Gold Standard			
		No stenosis	Stenosis <50%	Stenosis >50%	TOTAL
U-MRA	No stenosis	11	2		13
	Stenosis <50%	2	7	1	10
	Stenosis >50%		1	8	9
	TOTAL	13	10	9	32

Data presented are number of renal arteries. Sensitivity = 88.8%, Specificity = 95.65%, positive predictive value = 88.8%, negative predictive value = 95.65%, accuracy = 93,75%.

Table 3
Evaluation of the image quality of U-MRA by the two readers. Interobserver agreement.

	Image Quality		Interobserver agreement (κ value)
	Reader 1	Reader 2	
Overall	1.56 ± 1.08 [2]	1.68 ± 1.28 [2]	0.65
Main renal artery	1.63 ± 1.16 [2]	1.72 ± 1.28 [2]	0.69
Hiliar arteries	1.38 ± 1,08 [2]	1.54 ± 1.30 [2]	0.65
Intraparenchymal	0.86 ± 0.85 [1]	1.34 ± 1.19 [1]	0.51

Scores are means ± standard deviations, with medians in parentheses. Image quality was graded using a scale from 0 to 3 (3 = excellent, 2 = good, 1 = poor, 0 = non assessable).

Table 4
Summary of recent published literature using unenhanced magnetic resonance angiography sequences for renal artery assessment.

Author	Sequence	Number arteries	RAS	References standard	Sens. (%)	Spec. (%)
Gaudiano et al. [24]	3D Fiesta (fast imaging employing steady state precession, Siemens®)	186	36	CE-MRA or DSA	91.7	100
Xu et al. [17]	Inhance Inversion Recovery pulse GE®	126	33	CTA	100	99
Khoo et al. [21]	Inhance Inversion Recovery pulse GE®	149	21	CE-MRA	72,8	97,9
Albert et al. [20]	SSFP with time-spatial spin labeling pulse (time-SLIP, Toshiba®)	161	23	CTA	74	93
Utsunomiya et al. [16]	SSFP with time-spatial spin labeling pulse (time-SLIP, Toshiba®)	56	7/9	CTA/DSA	78	91
Braidy et al. [19]	3D balanced SSFP (True FISP, Siemens®)	114	17	CE-MRA	85	96
Parienty et al. [22]	SSFP with time-spatial spin labeling pulse (time-SLIP, Toshiba®)	45	36	DSA	93	88
Mohrs et al. [18]	3D balanced SSFP (True FISP, Siemens®)	76	20	CE-MRA	75	99
Maki et al. [23]	SSFP Philips®	83	20	CE-MRA	100	84

Fig. 2. (a) CE-MRA and (b) U-MRA depicted normal renal arteries in MIP axial reformatted images. Visualization of intraparenchymal arteries is easier by U-MRA because there is no parenchymal enhancement associated. Note that this coronal view is not achievable with DSA projections, this is one of the advantatges of MRA vs DSA.

signal-to-noise ratio. Arterial spin labeling (ASL) is a technique that can be combined with SSFP to enhance image quality through improved background tissue suppression. Protons upstream of the imaging field are "tagged" with an inversion pulse to provide contrast. Background tissue can be suppressed by subtracting the untagged image from the tagged blood image in two acquisitions or by applying a spatially nonselective tag pulse of the entire imaging field in addition to the tag pulse applied [13,15]. Recent studies have shown comparable results between U-MRA and CE-MRA, CTA and DSA in both healthy volunteers and patients with renal artery stenosis. These studies are summarized in Table 4 [16–24] (Figs. 2 and 3).

In our study, 12 of the 44 arteries imaged could not be evaluated using U-MRA, 10 because of respiratory artifacts or metallic vascular devices (4 renal artery stents and 2 aortic endophrostesis). These artifacts are not specific to U-MRU and they can also appear with the CE-MRE technique. Another artery could not be assessed due to bad positioning of the 3D volume, and the other was thin and thrombosed. In non-cooperative patients (movement and respiratory artifacts), patients of advanced age or patients with metallic devices, CTA with nephrotoxic or allergic prophylaxis, if necessary, is the technique of choice.

Seven of the nine polar and accessory arteries were correctly assessed with U-MRA. The remaining two accessory arteries were not visualized because they arose from the lower aorta near to the iliac bifurcation, out of the field of view of the U-MRA (Fig. 3). The limited craniocaudal coverage is a limitation that prevents this technique from being used in live kidney donors and in patients with anatomical variants of the kidneys such as horseshoe and pelvic kidneys. Failure to depict accessory renal arteries accounts for a considerable portion of false negative results in U-MRA studies [25].

Differentiating hemodynamic from non-hemodynamic stenosis is crucial because the former may require catheter-based revascularization (stent or dilatation) and the later can be managed conservatively. The four cases of our study that were misclassified with U-MRA from non stenosis to non hemodynamically significant stenosis cannot be considered as clinically relevant in terms of the therapeutic management. These controversial images corresponded to areas of kinking of the main renal arteries where evaluation is difficult even using the gold standard technique, and it is complicated to determine if there is a real stenosis or an angulated artery.

In the two cases where U-MRA classified hemodynamic stenosis as non-hemodynamic stenosis, the patients had renal artery FMD. In the two cases, there were multiple areas of stenosis and dilatations in the main renal arteries, making correct evaluation of renal arteries more challenging even for the gold standard techniques. There are only two articles available where FMD is depicted using U-MRA [23–25] (Fig. 4).

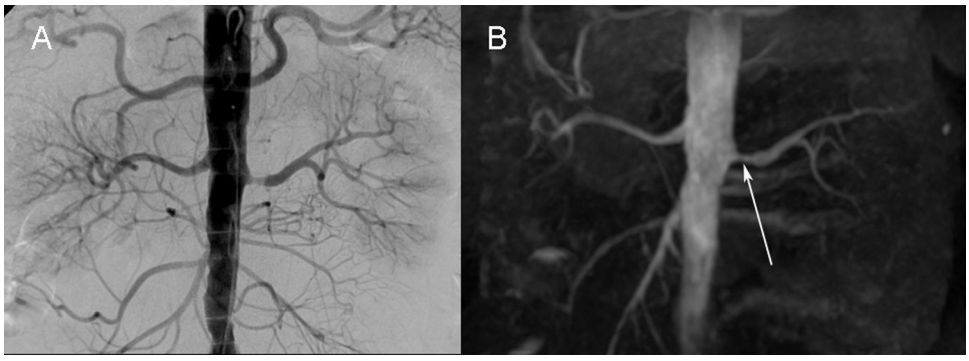

Fig. 3. (a) DSA and (B) U MRA MIP refformated image in a coronal view shows left main renal artery stenosis greater than 50%, balloon dilatation was performed in this case.

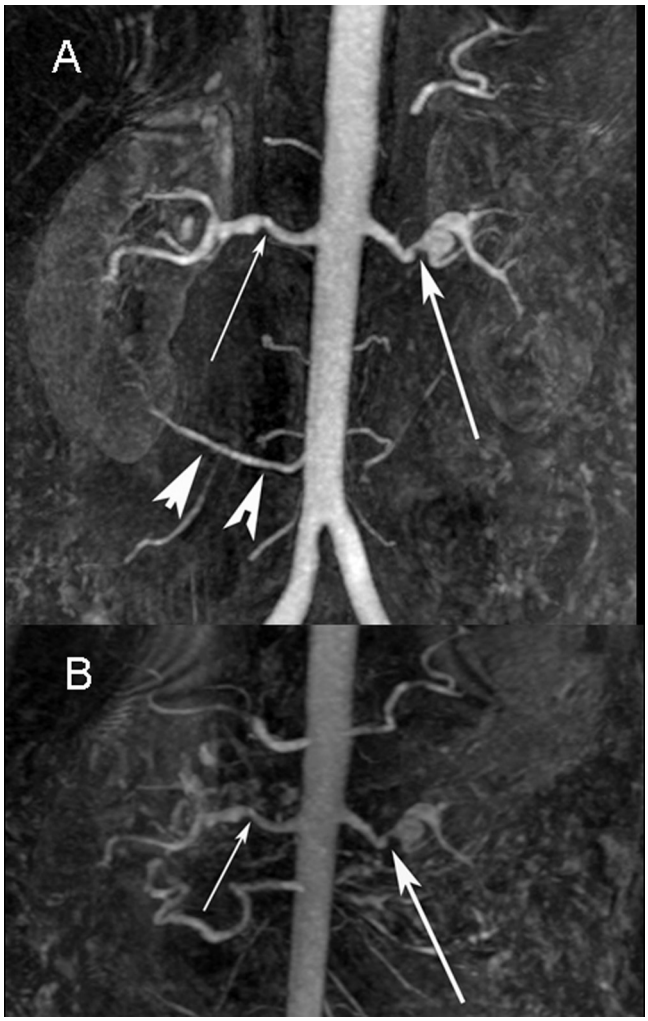

Fig. 4. (a) CE-MRA and (b) U-MRA depicts in a coronal view bilateral renal arteries FMD with more than 50% renal artery stenosis in the left renal artery (arrows), congruent between the two tests, and U-MRA pitfall in the right renal artery considering and hemodinamically significant artery by CE-MRA as non significant (thin arrows). Note a low aortic right accessory renal artery (arrowhead) in CE-MRA not seen in U-MRA.

The two readers considered the quality of visualization of main renal arteries in U-MRA images as "excellent" in 69% of the cases, diminishing these good results as thinner the arteries become. There is a tendency toward overestimation of stenoses in U-MRA caused by signal loss due to rapid, turbulent flow. In addition, the signal intensity of the blood immediately distal to a significant stenosis also decreases, thus, severe stenosis can be misinterpreted as occlusion (Fig. 5). Significant stenosis of the main renal artery also reduces the ability to visualize intraparenchymal arteries, being this the main cause of differences between the image quality scores for the main renal arteries and intraparenchymal arteries. Poor visualization of distal segment of hiliar and intrarenal arteries on CE-MRA and CTA is often due to suboptimal bolus timing and the masking of these segments by the enhanced renal parenchyma. Nevertheless, two of the advantages of U-MRA in the visualization of intraparenchymal arteries are the fact that the renal parenchymal does not enhance with U-MRA and the possibility to repeat the studies if the initial images are suboptimal. Calcification shows no signal on MR, this avoids the problem of differentiating calcium from contrast in heavily calcified stenosis as with CTA.

One limitation of this study is that the small number of patients included, and the fact that the imaging studies were performed

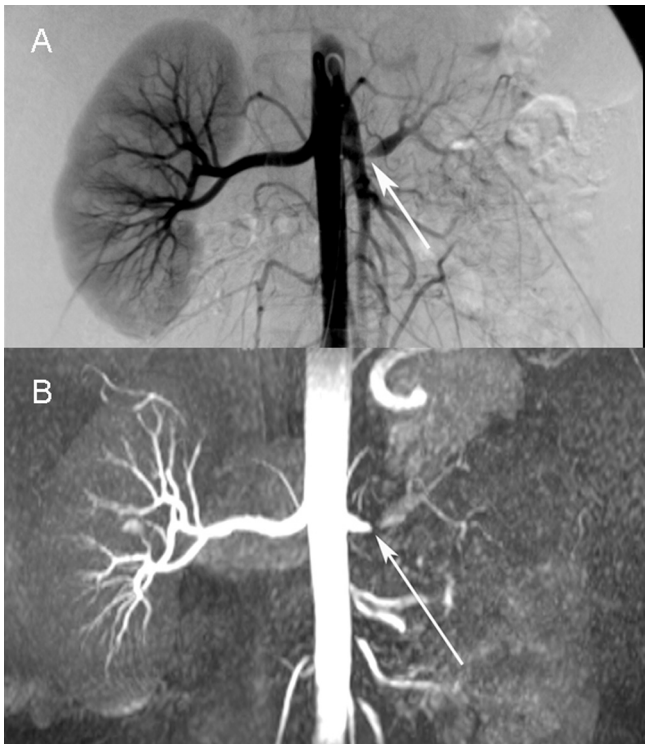

Fig. 5. (a) DSA and (b) U-MRA of a suboclusive left renal artery stenosis (arrows). Note that by U-MRA seems totally occlusive, although few distal intraparenchymal arteries are seen.

in a single institution, with low prevalence of hemodynamically significant RAS, and on a single MR scanner.

Another limitation is the fact that measurements of stenosis were made manually and not using an specific software. In addition, intraobserver and interobserver variability were not evaluated because we used a consensus approach for this study.

Other limitation of this study is the fact that CE-MRA was used as the reference standard in place of DSA, considered the gold standard. The tendency to overestimation of arterial stenosis on CE-MRA can constitute a bias in the results [20]. Although a recent article states that the stenotic degree of RAS was higher on CE-MRA than on U-MRA [26].

In conclusion, U-MRA can be used as an alternative to contrast-enhanced magnetic resonance angiography or computer tomography angiography in patients with renal insufficiency unless FMD is suspected. U-MRA may provide a safe alternative for evaluating stenosis of the renal arteries in patients with inconclusive ultrasonographic studies and patients in whom iodinated contrast or gadolinium injection is contraindicated. Nevertheless, when the finding is positive for FMD or arterial renal occlusion is depicted, the evaluation should be completed with an additional imaging modality to confirm and better assess the degree of stenosis.

Conflict of interest

None.

References

[1] K.J. Hansen, M.S. Edwards, T.E. Craven, et al., Prevalence of renovascular disease in the elderly: a population-based study, J. Vasc. Surg. 36 (2002) 443–451 http://www.ncbi.nlm.nih.gov/pubmed/12218965.
[2] B.R. Weber, R.S. Dieter, Renal artery stenosis: epidemiology and treatment, Int. J. Nephrol. Renovasc. Dis. (2014) 169–181 http://www.ncbi.nlm.nih.gov/pubmed/24868169.

[3] C.J. Cooper, T.P. Murphy, D.E. Cutlip, et al., Stenting and medical therapy for atherosclerotic renal-artery stenosis, N. Engl. J. Med. 370 (2014) 13–22 http://www.ncbi.nlm.nih.gov/pubmed/24245566.
[4] C.L. Paris, C.J. White, T.J. Collins, et al., Catheter-based therapy for atherosclerotic renal artery stenosis, Vasc. Med. 16 (2011) 109–112 http://www.ncbi.nlm.nih.gov/pubmed/21511673.
[5] C. Rountas, M. Vlychou, K. Vassiou, et al., Imaging modalities for renal artery stenosis in suspected renovascular hypertension: prospective intraindividual comparison of color Doppler US, CT, angiography, GD-enhanced MR angiography, and digital substraction angiography, Ren. Fail. 29 (2007) 295–302 http://www.ncbi.nlm.nih.gov/pubmed/17497443.
[6] J.K. Willmann, S. Wildermuth, T. Pfammatter, et al., Aortoiliac and renal arteries: prospective intraindividual comparison of contrast-enhanced three-dimensional MR angiography and multi-detector row CT angiography, Radiology 226 (2003) 798–811 http://www.ncbi.nlm.nih.gov/pubmed/12601190.
[7] S.B. Fain, B.F. King, J.F. Breen, et al., High-spatial-resolution contrast-enhanced MR angiography of the renal arteries: a prospective comparison with digital subtraction angiography, Radiology 218 (2001) 481–490 http://www.ncbi.nlm.nih.gov/pubmed/11161166.
[8] K.T. Tan, E.J.R. van Beek, P.W.G. Brown, et al., Magnetic resonance angiography for the diagnosis of renal artery stenosis: a meta-analysis, Clin. Radiol. 57 (2002) 617–624 http://www.ncbi.nlm.nih.gov/pubmed/12096862.
[9] F. Stacul, A.J. van Der Molen, P. Reimer, et al., Contrast induced nephropathy: updated ESUR contrast media safety committee guidelines, Eur. Radiol. 21 (2011) 2527–2541 http://www.ncbi.nlm.nih.gov/pubmed/21866433.
[10] J. Lee, J.Y. Cho, H.J. Lee, et al., Contrast-induced nephropathy in patients undergoing intravenous contrast-enhanced computed tomography in Korea: a multi-institutional study in 101487 patients, Korean J. Radiol. 15 (2014) 456–463.
[11] A. Canga, M. Kislikova, M. Martínez-Gálvez, et al., Renal function, nephrogenic systemic fibrosis and other adverse reactions associated with gadolinium-based contrast media, Nefrologia 34 (2014) 428–438 http://www.ncbi.nlm.nih.gov/pubmed/25036056.
[12] D.R. Broome, Nephrogenic systemic fibrosis associated with gadolinium based contrast agents: a summary of the medical literature reporting, Eur. J. Radiol. 66 (2008) 230–234 http://www.ncbi.nlm.nih.gov/pubmed/18372138.
[13] S. Morita, A. Masukawa, K. Suzuki, et al., Unenhanced MR angiography: techniques and clinical applications in patients with chronic kidney disease, Radiographics 31 (2011) E13–E33 http://www.ncbi.nlm.nih.gov/pubmed/21415179.
[14] G. Roditi, J.H. Maki, G. Oliveira, H.J. Michaely, Renovascular imaging in the NSF era, J. Magn. Reson. Imaging 30 (2009) 1323–1334 http://www.ncbi.nlm.nih.gov/pubmed/19937926.
[15] M.P. Hartung, T.M. Grist, C.J. François, Magnetic resonance angiography: current status and future directions, J. Cardiovasc. Magn. Reson. 13 (2011) 19 http://www.ncbi.nlm.nih.gov/pubmed/21388544.
[16] D. Utsunomiya, M. Miyazaki, Y. Nomitsu, et al., Clinical role of non-contrast magnetic resonance angiography for evaluation of renal artery stenosis, Circ. J. 72 (2008) 1627–1630 http://www.ncbi.nlm.nih.gov/pubmed/18728334.
[17] J.L. Xu, D.P. Shi, Y.L. Li, J.L. Zhang, et al., Non-enhanced MR angiography of renal artery using inflow-sensitive inversion recovery pulse sequence: a prospective comparison with enhanced CT angiography, Eur. J. Radiol. 80 (2011) e57–e63 http://www.ncbi.nlm.nih.gov/pubmed/20800405.
[18] O.K. Mohrs, S.E. Petersen, T. Schulze, et al., High-resolution 3D unenhanced ECG-gated respiratory-navigated MR angiography of the renal arteries: comparison with contrast-enhanced MR angiography, Am. J. Roentgenol. 195 (2010) 1423–1428 http://www.ncbi.nlm.nih.gov/pubmed/21098205.
[19] C. Braidy, I. Daou, A.D. Diop, et al., Unenhanced MR angiography of renal arteries: 51 patients, Am. J. Roentgenol. 199 (2012) w629–w637.
[20] T.S.E. Albert, M. Akahane, I. Parienty, et al., An international multicenter comparison of time-SLIP unenhanced MR angiography and contrast-enhanced CT angiography for assessing renal artery stenosis: the renal artery contrast-free trial, Am. J. Roentgenol. 204 (2015) 182–188 http://www.ncbi.nlm.nih.gov/pubmed/25539255.
[21] M.M.Y. Khoo, D. Deeab, W.M.W. Gedroyc, et al., Renal artery stenosis: comparative assessment by unenhanced renal artery MRA versus contrast-enhanced MRA, Eur. Radiol. 21 (2011) 1470–1476 http://www.ncbi.nlm.nih.gov/pubmed/21337034.
[22] I. Parienty, G. Rostoker, Jouniaux, et al., Renal artery stenosis evaluation in chronic kidney disease patients: nonenhanced time-spatial labeling inversion-pulse three-dimensional MR angiography with regulated breathing versus DSA, Radiology 259 (2011) 592–601 http://www.ncbi.nlm.nih.gov/pubmed/21330564.
[23] J.H. Maki, G.J. Wilson, W.B. Eubank, et al., Steady-state free precession MRA of the renal arteries: breath-hold and navaigator-gated techniques vs. CE-MRA, J. Magn. Reson. Imaging 26 (2007) 966–973 http://www.ncbi.nlm.nih.gov/pubmed/17896351.
[24] C. Gaudiano, F. Busato, E. Ferramosca, C. Cecchelli, B. Corcioni, L.B. De Sanctis, et al., 3D FIESTA pulse sequence for assessing renal artery stenosis: is it a reliable application in unenhanced magnetic resonance angiography, Eur. Radiol. 24 (2014) 3042–3050 http://www.ncbi.nlm.nih.gov/pubmed/25059677.
[25] Y. Pei, H. Shen, J. Li, et al., Evaluation of renal artery in hypertensive patients by unenhanced MR angiography using spatial labeling with multiple inversion pulses sequence and by CT angiography, AJR 199 (2012) 1142–1148 http://www.ncbi.nlm.nih.gov/pubmed/23096191.
[26] W. Zhang, J. Lin, S. Wang, et al., Unenhanced respiratory-gated magnetic resonance angiography (MRA) of renal artery in hypertensive patients using true fast imaging with steady-state precession technique compared with contrast-enhanced MRA, J. Comput. Assist. Tomogr. 38 (2014) 700–704 http://www.ncbi.nlm.nih.gov/pubmed/24733000.